TRANSITIONS TO CHAOTIC BEHAVIOR OF A FREQUENCY-PHASE LOCK SYSTEM

Valerie P. Ponomarenko
Research Institute of Applied Mathematics and Cybernetics,
Nizhni Novgorod, Russia,
povp@uic.nnov.ru

Nikolay N. Sorokin
Nizhegorodsky state university after N.I. Loachevski
Nizhni Novgorod, Russia

Abstract

The results of a numerical investigation of dynamical states and bifurcation transitions of a frequency-phase-feedback oscillator's model are presented in the paper. The behavior of the examined model is described by nonlinear six-dimensional set of differential equations with periodical nonlinearities. It is shown that the model demonstrates complex behavior including periodic and chaotic self-modulation oscillations, and various transitions to chaotic modes. Results are presented using one-parameter bifurcation diagrams, phase portraits of attractors, time realizations of oscillations, and Poincare maps.

Key words

Frequency-phase-feedback oscillator, regular and chaotic modes, synchronous regime, bifurcations and chaotic behavior, phase space, attractors, bifurcation diagrams, phase portraits, Poincare map.

1 Introduction

The systems with phase and frequency control are widely utilized in many electronic systems for solving the problems of stabilization, synchronization, and tracking. In these problems such systems provide for and automatically maintain the synchronous state, when the phase difference of reference and controlled signals becomes constant or, equivalently, the frequency difference of these signals is equal to zero [Shakhgil'dyan and Lyakhovkin, 1972]. The synchronous mode corresponds to a stable equilibrium state in the phase space of the corresponding system's dynamical model. The systems may also operate in nonsynchronous modes (modes with variable phase and frequency mismatches) corresponding to regimes of controlled oscillator with regular and chaotic frequency modulation. Feedback loops, when out-of-lock, provide broad possibilities for excitation of various nonsynchronous modes. By varying the parameters of control circuits, one can effectively govern the properties of generated oscillations and the domains where these oscillations exist. Thus, the system with phase and frequency control may be promising for devices where information is transmitted via chaotic signals. Therefore, knowledge of the specific features of the nonlinear dynamics for various systems versions is of significant importance.

The purpose of this paper is to present new results concerning the nonlinear dynamics of system with frequency-phase control combining phase-lock (PL) and frequency-lock (FL) partial subsystems. The system incorporates the controlled oscillator with two feedback loops including nonlinear discriminators of phase and frequency errors, low-frequency filters (LFFs) with transfer functions $K_1(p)$ and $K_2(p)$, and a frequency modulator [Kapranov, 1958]. We investigate nonsynchronous modes and its bifurcations of the frequency-phase lock (FPL) system in the case when each separate partial subsystem exhibits both regular and chaotic behavior.

2 Dynamical model of FPL system

The dynamic equation for phase difference φ between the controlled and reference signals in the FPL system is generally written in the form [Kapranov, 1958]:

$$p\varphi+\Omega K_1(p)F(\varphi)+\Omega_1 K_2(p)\Phi(p\varphi)=\delta\omega, \qquad (1)$$

Here $p\equiv d/dt$, $F(\varphi)$ and $\Phi(p\varphi)$ are the characteristics of phase and frequency discriminators normalized to unity; Ω and Ω_1 are the control circuit gains; and $\delta\omega$ is the initial frequency mistuning. Assume that the functions $F(\varphi)=sin\varphi$ and $\Phi(p\varphi)=2\beta_1 p\varphi/(1+\beta_1^2(p\varphi)^2)$ (β_1^{-1} is the frequency mistuning providing for the maximum value of $\Phi(p\varphi)$) approximate the phase and frequency discriminator characteristics respectively.

We will consider, according to problem formulation, FPL system with the second-order filter in PL subsystem and third-order filter in FL subsystem with transfer functions $K_1(p)=1/(1+(T_1+T_2)p+T_1T_2p^2))$, $K_2(p)=1/(1+$

$+(T_3+T_4+T_5)p+(T_3T_4+T_3T_5+T_4T_5)p^2+T_3T_4T_5p^3)$, where T_1, T_2,T_3,T_4, and T_5 are the inertia parameters. This case is of a special interest because the isolated partial FL subsystem with the third-order filter can possess a mode of two-spiral type chaotic attractor in its phase space, and the partial PL subsystem with the second-order filter individually exhibits chaotic modes of oscillatory (without of rotation of φ), rotatory, and oscillatory-rotatory types.

For considered LFFs equation (1) can be written in the form

$$\begin{gathered} d\varphi/d\tau=u,\ du/d\tau=z,\ dz/d\tau=v,\ dv/d\tau=w,\ dw/d\tau=\eta, \\ \mu_1\mu_2 d\eta/d\tau=\gamma-\sin\varphi-b\Phi(y)-(1+\varepsilon_2\cos\varphi)u- \\ -(\varepsilon_1+\varepsilon_2+\mu\cos\varphi+b\beta\varepsilon_1\Phi'(y))z-(\mu_1+\mu+\varepsilon_1\varepsilon_2+ \\ +\mu_2\cos\varphi+b\beta\mu_1\Phi'(y))v-(\mu_1\varepsilon_2+\varepsilon_1\mu+\mu_2)w-(\mu_1\mu+\varepsilon_1\mu_2)\eta+ \\ +\mu u^2\sin\varphi+\mu_2u^3\cos\varphi+3\mu_2uz\sin\varphi-b\beta^2\mu_1\Phi''(y)z^2, \end{gathered} \tag{2}$$

In equations (2) $\tau=\Omega t$ is the dimensionless time, $\gamma=\delta\omega/\Omega$,, $b=\Omega_l/\Omega$, $\beta=\beta_l\Omega$, $\mu=(T_3T_4+T_3T_5+T_4T_5)\Omega^2$, $\varepsilon_1=(T_1+T_2)\Omega$, $\varepsilon_2=(T_3+T_4+T_5)\Omega$, $\mu_1=T_1T_2\Omega^2$, $\mu_2=T_3T_4T_5\Omega^3$, $\Phi(y)=2y/(1+y^2)$, $\Phi'(y)=2(1-y^2)/(1+y^2)^2$, $\Phi''(y)=-4y(3-y^2)/(1+y^2)^3$, $y=\beta u$. Note that the system of equations (2) is phase dynamic system, it has the six-dimensional cylindrical phase space $U=\{\varphi(mod\ 2\pi),u,z,v,w,\eta\}$. Because of the system (2) nonlinearity its investigations are performed using qualitative-numerical methods of analysis of nonlinear dynamical systems [Belyustina, Kiveleva and Fraiman, 1982; Anishchenko, 1990] and employing the software developed in [Ponomarenko and Matrosov, 1997]. In the course of analysis, we examined time realizations, projections attractor's phase portraits, Poincare maps, and one-parameter bifurcation diagrams.

3 Stability of the synchronous mode

First, let us establish stability conditions for the synchronous mode. At $0\le\gamma<1$, system (2) has two equilibrium states: $A_1(arcsin\gamma,\ 0,0,0,0,0)$ and $A_2(\pi-arcsin\gamma,\ 0,\ 0,0,0,0)$. The equilibrium state A_1 may be both stable and unstable, and A_2 is an unstable saddle type equilibrium state. We find stability conditions for equilibrium state A_1 by analyzing the roots of the characteristic equation for the eigenvalues of the linearized system near A_1

$$\lambda^6+a_1\lambda^5+a_2\lambda^4+a_3\lambda^3+a_4\lambda^2+a_5\lambda+a_6=0. \tag{3}$$

In equation (3)

$$\begin{gathered} a_1=(\mu\mu_1+\mu_2\varepsilon_1)/\mu_1\mu_2,\ a_2=(\mu_1\varepsilon_2+\mu_2+\varepsilon_1\mu)/\mu_1\mu_2, \\ a_3=(\varepsilon_1\varepsilon_2+\mu+\mu_1+\mu_2(1-\gamma^2)^{1/2}+2b\beta\mu_1)/\mu_1\mu_2, \\ a_4=(\varepsilon_1+\varepsilon_2+\mu(1-\gamma^2)^{1/2}+2b\beta\varepsilon_1)/\mu_1\mu_2, \\ a_5=(1+\varepsilon_2(1-\gamma^2)^{1/2}+2b\beta)/\mu_1\mu_2,\ a_6=(1-\gamma^2)^{1/2}/\mu_1\mu_2. \end{gathered}$$

The stability conditions can be written in the form

$$\begin{gathered} a_1,a_2,\ \dots\ ,a_6>0,\ a_3(a_1a_2-a_3)-a_1(a_1a_4-a_5)>0, \\ (a_1a_2-a_3)[a_5(a_4a_3-a_2a_5)+a_6(2a_1a_5-a_3^2)]+ \\ +(a_1a_4-a_5)[a_1a_3a_6-a_5(a_1a_4-a_5)]-a_1^3a_6^2>0. \end{gathered} \tag{4}$$

If conditions (4) are satisfied, the studied FPL system has a synchronous mode corresponding to equilibrium state A_1. The domain of parameters C_s where conditions (4) are fulfilled corresponds to the domain where synchronous mode persists. When as a result of parameters varying, conditions (4) are violated limit cycle of oscillatory type during which the φ coordinate is not exceed 2π arises in the phase space U. This limit cycle corresponds to a quasi-synchronous mode in the FPL system where periodic oscillations of phase variables are observed around equilibrium state A_1 that has become unstable.

4 Dynamical modes and bifurcations of model (2)

Now let us consider nonsynchronous modes of the FPL system that develops for the parameter values out of domain C_s. For this purpose, we use the results of numerical simulation of model (2).

Fig.1 displays one-parameter bifurcation diagram $\{\mu_1,\varphi\}$ for the point Poincare mapping produced by the trajectories of model (2). The diagram is calculated at the parameter values $\gamma=0.55$, $b=1$, $\beta=20.5$, $\varepsilon_1=1.25$, $\varepsilon_2=15$, $\mu=2$, $\mu_2=3.2$. Fig.2 shows (φ,u) projections of the phase portraits, (φ,v) and (z,v) projections of the Poincare map, and time realization $u(\tau)$ corresponding to the attractors of model (2). The $\{\mu_1,\varphi\}$ diagram depicts evolution of quasi-synchronous modes of limit cycles S_1 (Fig.2*a*) and S_2 (Fig.2*d*) as parameter μ_1 varies from 1.8 to 8.11. Note, that in the interval $1.8<\mu_1<3.0$ the bistable behavior of the system is observed; i.e., the attractors based on limit cycles S_1 and S_2 exist in the phase space simultaneously. One can see that the mode of cycle S_2 becomes chaotic (Fig.2*h*) via period-doubling bifurcations; then, the mode of chaotic attractor P_2 is destroyed, and the system passes to the mode of complex limit cycle S^* (Fig.2*i*).

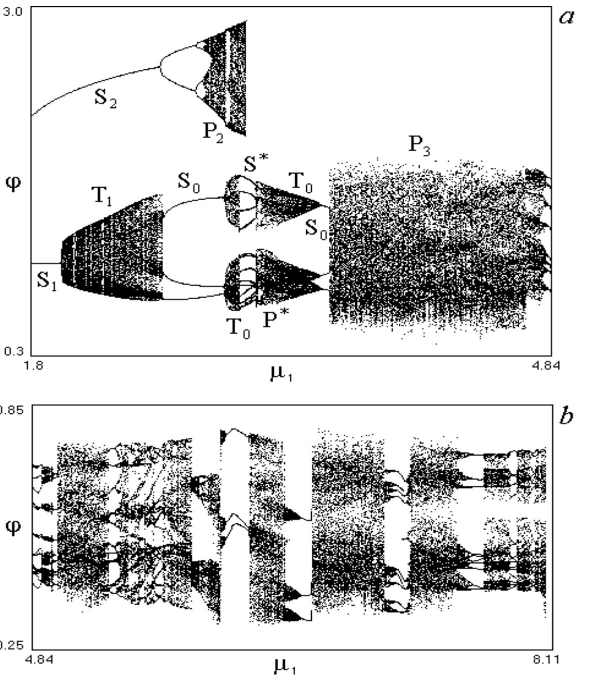

Fig. 1. Bifurcation diagram $\{\mu_1,\varphi\}$

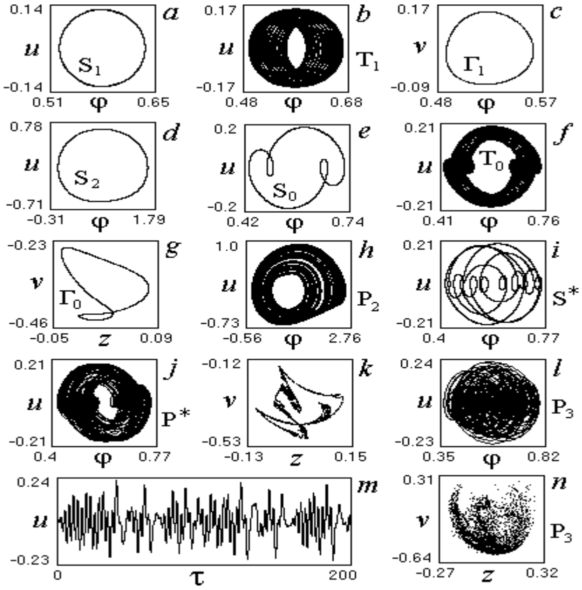

Fig. 2. Phase portraits (a,b,d-f,h-j,l), Poincare map (c,g,k,n), and time realization $u(\tau)$ corresponding to attractors of model (2)

The evolution of the mode of cycle S_1, as μ_1 is increased, starts when a stable limit cycle S_1 becomes unstable and gives rise to a stable 2D torus T_1 (Fig.2b). In Fig.2c close invariant curve Γ_1 of the Poincare map corresponding to the torus T_1 is given. With increasing μ_1 the mode of torus T_1 collapses, and the system passes to the mode of oscillatory limit cycle S_0 (Fig.2e). With a further increase of μ_1 the mode of torus T_0 from the limit cycle S_0 appears (Figs.2f, 2g) which than, is rigidly replaced by the mode of complex oscillatory limit cycle S^* (fig.2i). Then, the cycle S^* breaks down and the system rigidly enters a mode of oscillatory type chaotic attractor P^* (Figs.2j, 2k). As μ_1 is increased attractor P^* is softly transformed to the torus T_0, which further is transformed to limit cycle S_0, and the system again returns to the periodic quasi-synchronous mode. When $\mu_1>3.54$ the mode of cycle S_0 is rigidly replaced by the mode of oscillatory type chaotic attractor P_3 (Figs.2l-2n). In interval $4.69<\mu_1<8.3$ irregular alternation of chaotic, periodic, and quasi-synchronous modes is observed. When μ_1 passes through the value $\mu_1=8.33$, the system passes to the asynchronous (with rotation of φ) mode of oscillatory-rotatory type chaotic attractor via intermittency.

Fig.3 represents bifurcation diagram $\{\gamma,\varphi\}$ corresponding to the parameter values $b=1$, $\beta=20.5$, $\varepsilon_1=1.25$, $\varepsilon_2=15$, $\mu=2$, $\mu_1=6.25$, $\mu_2=3.2$. It characterizes evolution of quasi-synchronous modes that develop in the system on the base of the mode of limit cycle S_1 when γ decreases. It is seen from the diagram that alternating modes of torus T_1, limit cycle S_3, torus T_3, chaotic attractor P_4, limit cycle S_4, torus T_4, chaotic attractor P_5, and limit cycle S_5 are observed in the model (2). Fig.4 displays (φ,u) projections of the phase portraits, time realizations $\varphi(\tau)$ and $u(\tau)$, and (φ,v) and (z,u) projections of the Poincare map corresponding to these modes.

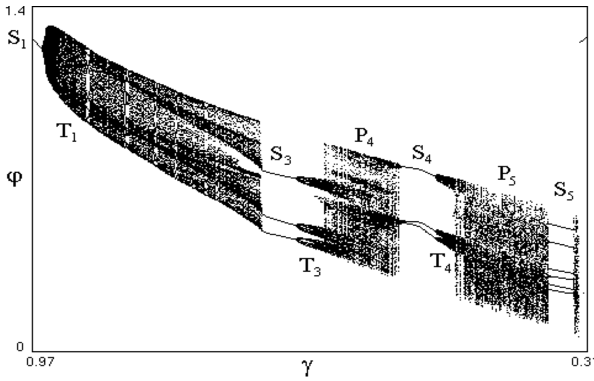

Fig. 3. Bifurcation diagram $\{\gamma,\varphi\}$

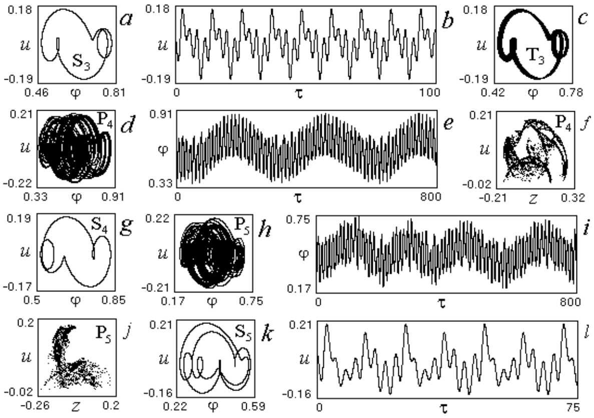

Fig. 4. Phase portraits (a,c,d,g,h,k), Poincare map (f,j), and time realizations $\varphi(\tau)$ and $u(\tau)$ corresponding to attractors of model (2)

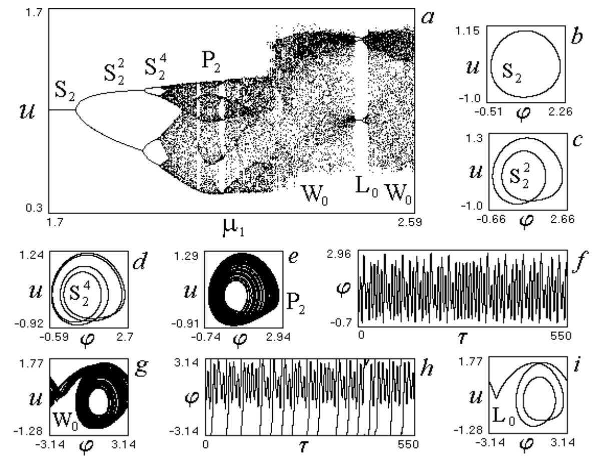

Fig. 5. Evolution of quasi-synchronous mode with increasing of μ_1

The bifurcation diagram $\{\mu_1,u\}$ represented in Fig.5a shows transformation of quasi-synchronous mode of the limit cycle S_2 into asynchronous mode of oscillatory-rotatory type chaotic attractor W_0. The diagram calculated at the parameter values $\gamma=0.5$, $b=0.5$, $\beta=1$, $\varepsilon_1=0.9$, $\varepsilon_2=80$, $\mu=2$, $\mu_2=2$. Figs.5b-5i display (φ,u) projections of the phase portraits, and time realizations $\varphi(\tau)$ corresponding to oscillatory and oscillatory-rotatory attractors of the system. With increasing of μ_1 limit cycle S_2 is softly transformed into chaotic attractor

P_2 through period doubling bifurcations (Figs.5*b*-5*f*). With further increasing of μ_1 attractor P_2 is transformed into chaotic attractor W_0 (Figs.5*g*, 5*h*). Then there is a "window" of values of μ_1 at $\{\mu_1,u\}$ diagram corresponding to the mode of oscillatory-rotatory type limit cycle L_0 (Fig.5*i*).

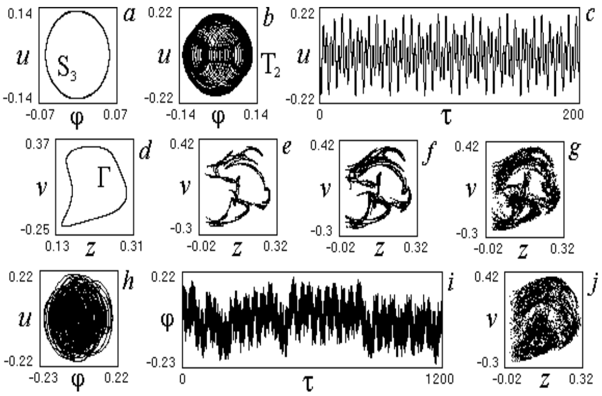

Fig. 6. Transition to the chaotic quasi-synchronous mode via torus distortion

Formation of chaotic quasi-synchronous mode may be realized in the system considered via distortion of the oscillatory torus mode. This effect is illustrated by (φ,u) projections of the phase portraits, time realizations $\varphi(\tau)$ and $u(\tau)$, and (z,v) projections of the Poincare map represented at Fig.6 for the parameter values γ=0, b=1, β=20.5, ε_2=15, μ=2, μ_1=3.7, μ_2=3.2. Fig.6 shows evolution of quasi-synchronous mode of limit cycle S_3 (Fig.6*a*) when parameter ε_1 decreases from 1.2 to 0.72. When ε_1 decreases the mode of oscillatory torus T_2 (Figs.6*b*-6*d*) appears from limit cycle S_3. After torus T_2 is formed, the phase portrait of the Poincare map (Fig.6*d*) is characterized by the presence of stable closed invariant curve Γ. With decreasing of ε_1 the distortion of the curve Γ and gradual transformation of the mode of torus-chaos type chaotic attractor (Figs.6*e*-6*j*) takes place.

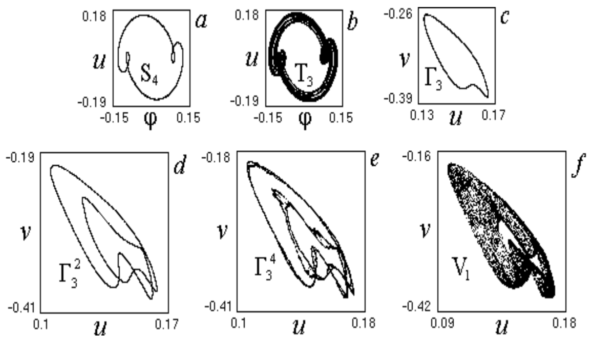

Fig. 7. Formation of oscillatory type chaotic attractor via torus-doubling bifurcation

The model (2) exhibits such interesting phenomena as formation of oscillatory type chaotic attractor via torus-doubling bifurcation, and rise of 3D torus in the phase space U. Fig.7 illustrates the first of these phenomena. It shows (φ,u) projections of the phase portraits, (φ,v) and

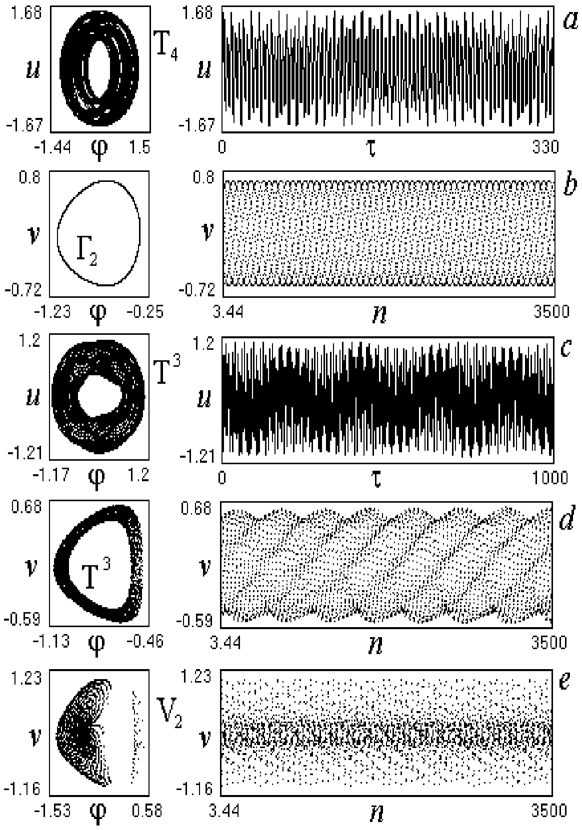

Fig. 8. Rise the mode of 3D torus and transition to a chaotic mode

(u,v) projections of the Poincare map corresponding to the attractors of model (2) for the parameter values γ=0, b=1, β=20.5, ε_2=15, μ=2, μ_1=3.7, μ_2=3.2. Parameter ε_1 decreases from 1.65 to 1.45. For ε_1=1.65 the mode of oscillatory limit cycle S_4 (Fig.7*a*) is the initial state of the system. We see that, as ε_1 decrease, cycle S_4 losses its stability, and torus T_3 (Fig.7*b*) corresponding to closed invariant curve Γ_3 (Fig.7*c*) appears in the phase space. Then period doubling bifurcations of curve Γ_3 adequate to torus-doubling bifurcations occurs with formation of closed invariant curves Γ_3^2 and Γ_3^4 (Figs.7*d*, 7*e*). If ε_1 continues to decrease, the mode of chaotic attractor V_1 rises.

Fig.8 exhibit the second of above-mentioned phenomena. It displays the results of numerical simulation of model (2) for the parameter values γ=0.01, b=5, β=1, ε_1=1, ε_2=35, μ=2.5, μ_2=3.2, when parameter μ_1 varies from 1.34 to 1.537. These results are presented in the form of (φ,u) projections of the phase portraits, (φ,v) projections of the Poincare map, time realizations $\varphi(\tau)$ and $u(\tau)$, and dependences $v(n)$, where n is the number of the Poincare cross-section point. Let us consider the quasi-synchronous mode of torus T_4 (Fig.8*a* corresponding to closed invariant curve Γ_2 (Fig.8*b*) as the system's initial state. When μ_1 grows the mode of 3D torus T^3 appears (Figs.8*c*, 8*d*). Then, transition to the mode of chaotic attractor V_2 is observed (Fig.8*e*).

The model (2) also exhibits interesting phenomenon of formation of oscillatory type chaotic attractor that is

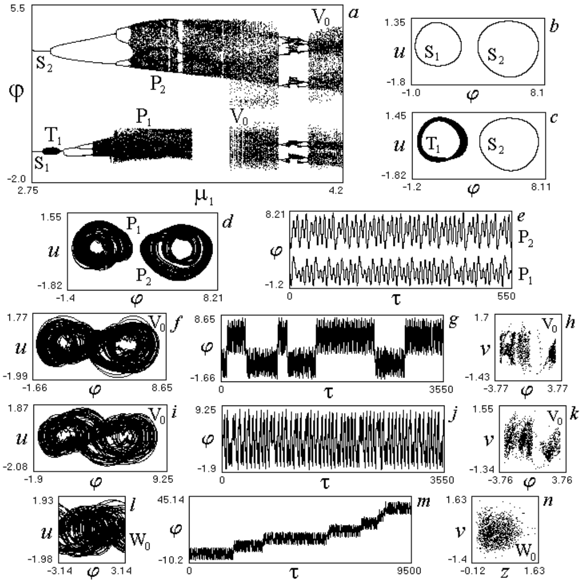

Fig. 9. Formation of oscillatory type chaotic attractor with irregular switches of a phase variable φ.

characterized by irregular switches of a phase variable φ. Fig.9a represents bifurcation diagram $\{\mu_1,\varphi\}$ corresponding to γ=0.15, b=5, β=1, ε_1=1, ε_2=35, μ=2.5, μ_2=13.5. Figs.9*b*-9*n* shows (φ,*u*) projections of the phase portraits, time realizations $\varphi(\tau)$, and (φ,*v*) and (*z*,*v*) projections of the Poincare map corresponding to the system's attractors, when parameter μ_1 varies from 2.75 to 4.98. The modes of limit cycles S_1 and S_2 (Fig.9*b*) are the system's starting state for μ_1=2.75. The $\{\mu_1,\varphi\}$ diagram shows how the modes of cycles S_1 and S_2 become chaotic via period doubling bifurcations corresponding to attractors P_1 and P_2 (Figs.9*c*-9*e*). When μ_1 increases the system passes to the mode of chaotic attractor V_0, characterized by irregular alternating oscillations at the attractors P_1 and P_2 (Figs.9*f*-9*h*). The dynamic φ range of attractor V_0 exceeds 2π. Formation of attractor V_0 indicates that, in the phase space, there are two domains where the system chaotically oscillates and irregularly passes from one domain into the other. As μ_1 increases the duration of oscillations in these domains decrease, while the frequency of switches from one domain to another grows (Figs.9*i*-9*k*). Then, the system undergoes a hard transition to the asynchronous mode of oscillatory-rotatory type chaotic attractor W_0 (Figs.9*l*-9*n*).

5 Conclusion

In this paper we have investigated the dynamical modes and transitions to the chaotic behavior in a frequency-phase locked system with the second-order filter in a phase-locked loop and the third-order filter in a frequency-locked loop. Using the dynamical model of considered FPL system we found that the system exhibit's a rich variety of nonsynchronous modes: periodic modes caused by the loss of the synchronous mode stability and by saddle-node bifurcations of oscillatory limit cycles; quasi-periodic quasi-synchronous modes corresponding to oscillatory 2D and 3D tori in the phase space; chaotic modes that formed via period-doubling bifurcations, as well as rigidly formed through saddle-node bifurcations of limit cycles, via destruction of tori, via the torus-doubling bifurcations, via the creation of united chaotic attractor in the phase space with irregular switches of phase variable φ.

These phenomena, in our opinion, are of importance for both basic and applied research of nonlinear dynamics of the system with frequency and phase control. It further to understanding the behavior of the systems when the synchronous state is cut off as a result of the system parameters perturbation. The discovered effects of nonlinear dynamics and the obtained data on restructuring FPL system's dynamical states under variation of the system's parameters are of interest for suppression or enhancement of mode instabilities, control of behavior modes, and generation of chaotic oscillations.

The wide variety of chaotic modes offers considerable possibilities of forming various frequency-modulated signals at the output of the FPL system. Control the characteristics of generated signals can be easily realized by means of subsystems parameters.

Acknowledgements

This work was supported by the Russian Foundation for Basic Research (grants No 05-02-17409, No 06-02-16499).

References

Shakhgil'dyan, V. V. and Lyakhovkin, A. A. Phase-Lock Systems (Svyaz', Moscow, 1972) [in Russian].

Kapranov, M. V. Nauch. Dokl. Vyssh. Shkoly, Radiotekh. Electron. 2 (9), p. 162 (1958) [in Russian]..

Belyustina, L. N., Kiveleva, K. G., and Fraiman, L. A. Phase-Lock Systems. Ed. by V. V. Shakhgil'dyan and L. N. Belyustina (Radio i Svyaz', Moscow, 1982), p. 21 [in Russian].

Anishchenko, V. S. Complex Oscillation in Simple Systems (Nauka, Moscow, 1990) [in Russian].

Ponomarenko, V.P. and Matrosov, V.V. Vestn. Verkhne-Volzhskogo otdeleniya ATN RF. Vysokie tekhnologii v radioelektronike. N. Novgorod. No. 2(4), p. 15 (1997) [in Russian].